

## In-Plane and Out-of-Plane Infrared Difference Spectroscopy Unravels Tilting of Helices and Structural Changes in a Membrane Protein upon Substrate Binding

Víctor A. Lórenz-Fonfría,<sup>\*,†</sup> Meritxell Granell,<sup>†</sup> Xavier León,<sup>†,§</sup> Gérard Leblanc,<sup>‡</sup> and Esteve Padrós<sup>†</sup>

Unitat de Biofísica, Departament de Bioquímica i de Biologia Molecular, and Centre d'Estudis en Biofísica, Universitat Autònoma de Barcelona, 08193 Bellaterra, Barcelona, Spain, and Institut de Biologie et Technologies-Saclay, Service de Bioénergétique, Biologie Structurale et Mécanismes, CEA-Saclay, F-91191 Gif sur Yvette, France

Received July 28, 2009; E-mail: victor.lorenz@gmail.com

The characterization of conformational changes triggered by the interaction of substrates/ligands with membrane proteins is an essential step toward understanding both molecule transport and signal transduction in cells. A steadily growing number of X-ray crystallographic atomic models of secondary transporters hold promise for revealing the structural basis of their transport mechanisms.<sup>1</sup> To date, however, only for lactose permease have X-ray structures been solved for both ligand-free and ligand-bound forms.<sup>2</sup> They reveal few structural changes localized in the binding pocket, which contrasts with the results of studies under more functional conditions that suggest major changes in the tilt of helices upon lactose binding.<sup>3</sup> This example highlights the need for structural methods alternative to X-ray crystallography that are able to assay substrate-induced changes under conditions as physiological as possible, ideally without using potentially perturbing probes. Here we present a spectroscopic approach fulfilling these requirements that is based on a change of coordinates allowing the computation of infrared (IR) difference spectra in and out of the plane of an attenuated total reflection (ATR) crystal from polarized data. Spectroscopic rules for unequivocally discriminating between changes in the tilt of transmembrane helices and other structural rearrangements are also introduced. We have applied the present method to characterize the structural changes in the secondary transporter melibiose permease (MelB) from *Escherichia coli* driven by the binding and transport of the disaccharide melibiose.

IR difference spectroscopy stands out because of its ability to monitor changes in protein backbone and amino acid side chains in membrane proteins in a preserved lipid environment without the need for external probes.<sup>4</sup> Near-physiological conditions in terms of hydration, ionic strength, and temperature can be attained in the ATR mode, where precise control of the buffer medium is trivial. In IR difference spectroscopy, a reconstituted membrane protein is switched between two states (e.g., from **A** to **B**) by either light, an electrochemical potential, or (as done here) alternation of buffers without and with substrates. An IR difference spectrum is obtained and corrected for all nonspecific changes.<sup>5</sup> Negative and positive peaks emerge as a result of changes in the frequency and/or intensity of the transition dipole moments, **M**, of the different vibrations in going from **A** to **B**. This is caused either by chemical changes (e.g., deprotonation of a carboxylic group), environment changes (e.g., a change in the H-bonding strength), or conformational changes (e.g., a change in the vibrational coupling of the peptide bond), providing the grounds for the interpretation of IR difference spectra in structural terms.<sup>4</sup>

The stacked disposition of the sample in the ATR crystal plane (*x,y* in Figure 1) makes ATR-IR difference spectra also sensitive to changes in the orientation of **M** with respect to the ATR surface normal (the *z* direction) even when unpolarized IR light is used.<sup>6</sup> However, this

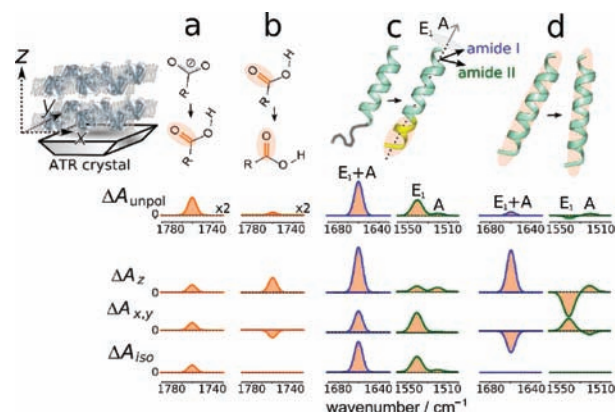


**Figure 1.** Schematic representation of the origins of bands in IR difference spectra of axially distributed reconstituted protein samples: (a) deprotonation and (b) reorientation of one carboxylic group; (c) elongation and (d) reorientation of one helix. The displayed intensities for  $\Delta A_{\text{unpol}}$  correspond to unpolarized light with a Ge crystal ( $n_1 \approx 4$ ). The bottom part shows the corresponding  $\Delta A_z$ ,  $\Delta A_{x,y}$ , and  $\Delta A_{\text{iso}}$  values. Negative bands from the lost carboxylate group in (a) and from the lost loop structure in (c) have been omitted for clarity. For further details, see the SI.

sensitivity is habitually insufficient for beneficial use but can be intense enough to complicate the interpretation of the difference spectra. As simulated in Figure 1 for a Ge crystal, both the protonation of a carboxylic group (Figure 1a) and its reorientation (Figure 1b) give rise to positive bands in unpolarized difference spectra, although the latter is much less intense [but see Figure S1 in the Supporting Information (SI) for a different ATR crystal]. Equivalently, both the elongation of a helix (Figure 1c) and a decrease in its tilt (Figure 1d) give rise to positive bands at the amide I vibration frequency expected for transmembrane helices. The behavior of the amide II vibration is more complex as a result of two orthogonal split modes (A and  $E_1$ ).

Through the use of parallel and perpendicular polarized light, nonisotropic samples with axial symmetry can be appropriately characterized.<sup>7</sup> However, it has been shown that substrate-induced polarized difference spectra,  $\Delta A_{\parallel}$  and  $\Delta A_{\perp}$ , are difficult to interpret.<sup>8</sup> In contrast, difference spectra along the *z* axis and in the *x,y* plane would allow for a more straightforward structural interpretation. The different behavior of  $\Delta A_z$  and  $\Delta A_{x,y}$  allow the discrimination of bands originating from changes in vibration frequencies (or intensities), characterized by identical signs for  $\Delta A_z$  and  $\Delta A_{x,y}$  (Figure 1a,c), from those arising from pure reorientation changes, which have opposite signs for  $\Delta A_z$  and  $\Delta A_{x,y}$  (Figure 1b,d). Furthermore, the isotropic difference spectrum (Figure 1), which is free from reorientation-related effects, can then be easily computed as  $\Delta A_{\text{iso}} = \Delta A_z + 2\Delta A_{x,y}$ .<sup>6</sup> In contrast, the use of  $\Delta A_{\text{unpol}}$ , or even  $\Delta A_{\parallel}$  and  $\Delta A_{\perp}$ , leads to mixed bands coming from both reorientation and environmental changes.

As described in a different context,<sup>6</sup> in an ATR setup,  $\Delta A_z$  and  $\Delta A_{x,y}$  can be obtained by combination of  $\Delta A_{\parallel}$  and  $\Delta A_{\perp}$  as follows:

<sup>†</sup> Universitat Autònoma de Barcelona.

<sup>‡</sup> Institut de Biologie et Technologies-Saclay.

<sup>§</sup> Present address: Centre de Biotecnologia Animal i Teràpia Gènica, Universitat Autònoma de Barcelona.

$$\Delta A_{x,y} = \Delta A_{\perp} / E_y^2$$

$$\Delta A_z = (\Delta A_{\parallel} - \Delta A_{\perp} E_x^2 / E_y^2) / E_z^2 \quad (1)$$

where  $\mathbf{E} = (E_x, E_y, E_z)$  is the electric field vector of the ATR evanescent wave normalized to the incident wave, computed here using the thick-film hypothesis.<sup>9</sup> Equation 1 was further modified to take into account the polarizer leak fraction (see the SI).

We applied these concepts to the substrate-induced IR difference spectra of MelB, a membrane protein that is able to couple the active transport of melibiose to the electrochemical gradient of each of three different cations ( $H^+$ ,  $Na^+$ , or  $Li^+$ ).<sup>10</sup> The MelB was purified and reconstituted in *E. coli* lipids as described elsewhere.<sup>5</sup> Figure 2a shows difference spectra induced by melibiose in the presence of  $Na^+$  obtained by repetitively cycling buffers without and with melibiose<sup>5</sup> and alternating parallel- and perpendicular-polarized light during the acquisition (see Figure S3).

The computed  $\Delta A_z$  and  $\Delta A_{x,y}$  are shown in Figure 2b (original spectra), and their uncertainties are displayed in Figure S2. We will focus the discussion on the amide I bands, which are more informative and straightforward to interpret than the amide II bands. The most remarkable feature is the opposite sign of  $\Delta A_z$  and  $\Delta A_{x,y}$  at  $\sim 1665$ – $1655$   $cm^{-1}$ , with  $\Delta A_{iso}$  close to zero at  $\sim 1658$   $cm^{-1}$  (Figure 2b original), suggesting from the wavenumber and the intensity pattern the reorientation of some transmembrane helices (compare with Figure 1d left). However, the band broadening intrinsic to IR spectroscopy precludes a clear resolution of the component bands.

We applied a maximum-entropy deconvolution method<sup>11</sup> to mathematically reduce the width of the bands in the difference spectra (Figure 2b, narrowed spectra). After this, a completely resolved peak at  $1658$   $cm^{-1}$  appeared in both  $\Delta A_z$  and  $\Delta A_{x,y}$  (red dashed box in Figure 2b), and its assignment to a reduced tilt of some helices became clear, as it fulfilled the intensity pattern for  $\Delta A_z$ ,  $\Delta A_{x,y}$ , and  $\Delta A_{iso}$  shown in Figure 1d. This same band was previously resolved as a positive peak<sup>5</sup> (i.e., reorientation of groups contributes to the unpolarized difference absorbance), as we illustrated in Figure 1.

Interestingly, the peak at  $1658$   $cm^{-1}$  was recently found to be absent in a mutant that binds but does not transport melibiose,<sup>12</sup> clearly suggesting that the detected helix tilt is associated not with the sugar-binding process but with the following sugar/cation cotransport. The observed reduction of the tilt of some helices of MelB most likely reflects the formation of the so-called occluded state (Figure 2b inset), one of the proposed intermediate states by which secondary transporters may alternate access to the substrate binding site from either side of the membrane.<sup>1</sup>

We should also note that the same sign is observed in both  $\Delta A_z$  and  $\Delta A_{x,y}$  for the rest of the bands in the amide I region ( $\sim 1700$ – $1620$   $cm^{-1}$ ). The same holds for the bands in the amide II region ( $\sim 1580$ – $1510$   $cm^{-1}$ ), which reports more averaged structural changes because of its lower structure sensitivity. The detected decrease in the tilt of some helices should therefore be accompanied by an important structural reorganization (e.g., elongation/disruption of helices/loops). For instance, the positive peak at  $1667$   $cm^{-1}$  shows higher intensity in  $\Delta A_z$  than in  $\Delta A_{x,y}$  and is likely to originate from the elongation of some transmembrane helices with low tilt upon melibiose binding, in accordance with Figure 1c.

In summary, the study and interpretation of the structural changes in membrane proteins upon substrate binding is simplified by computing  $\Delta A_z$ ,  $\Delta A_{x,y}$ , and  $\Delta A_{iso}$  from polarized IR difference spectra. In combination with simple rules and band-narrowing methods, it can allow structural and orientation changes induced by substrate binding to be disentangled. Further structural and functional insights are possible if this method is combined with

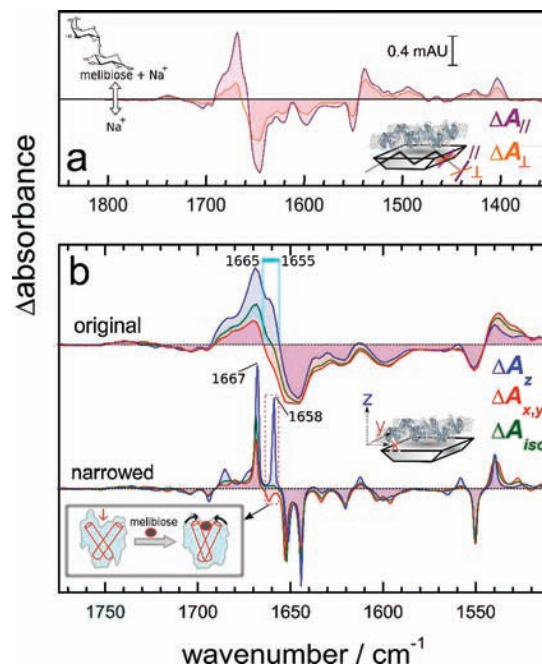


**Figure 2.** (a) Melibiose-induced polarized IR difference spectra of MelB reconstituted in *E. coli* lipids in the presence of  $Na^+$  [10 mM NaCl, 100 mM KCl, 20 mM MES (pH 6.6)] using 10 mM melibiose. Difference spectra were obtained with a KRS polarizer at 4  $cm^{-1}$  resolution with 16 000 averaged scans each. (b) Calculated difference spectra along the  $z$  axis (blue) and in the  $x,y$  plane (red) obtained as  $\Delta A_z = 0.410\Delta A_{\parallel} - 0.360\Delta A_{\perp}$  and  $\Delta A_{x,y} = 0.454\Delta A_{\perp} - 0.011\Delta A_{\parallel}$ , respectively. The original difference spectra were mathematically narrowed as described in ref 5. The calculated  $\Delta A_{iso}$  spectrum is shown in green. The inset shows the molecular interpretation of the intensity pattern of the band at  $\sim 1658$   $cm^{-1}$ .

site-directed mutagenesis or isotopic labeling. The present approach can be also useful in the structural interpretation of light- and potential-induced IR difference spectra of proteins.

**Acknowledgment.** This work was supported by UAB Postdoctoral Fellowship 40607 and Marie Curie Reintegration Grant PIRG03-6A-2008-231063 (to V.A.L.-F.) and by Dirección General de Investigación Grant BFU2006-04656/BMC (to E.P.).

**Supporting Information Available:** Figures S1–S3 and methods for computing the intensities in Figure 1 and estimating  $\Delta A_z$  and  $\Delta A_{x,y}$  from  $\Delta A_{\parallel}$  and  $\Delta A_{\perp}$ , taking into account the polarizer leak. This material is available free of charge via the Internet at <http://pubs.acs.org>.

## References

- (1) DeFelice, L. J. *Trends Neurosci.* **2004**, *27*, 352. Karpowich, N. K.; Wang, D. N. *Science* **2008**, *321*, 781. Diallinas, G. *Science* **2008**, *322*, 1644.
- (2) Abramson, J.; Smirnova, I.; Kasho, V.; Verner, G.; Kaback, H. R.; Iwata, S. *Science* **2003**, *301*, 610. Mirza, O.; Guan, L.; Verner, G.; Iwata, S.; Kaback, H. R. *EMBO J.* **2006**, *25*, 1177.
- (3) Smirnova, I.; Kasho, V.; Choe, J. Y.; Altenbach, C.; Hubbell, W. L.; Kaback, H. R. *Proc. Natl. Acad. Sci. U.S.A.* **2007**, *104*, 16504. Zhou, Y.; Guan, L.; Freitas, J. A.; Kaback, H. R. *Proc. Natl. Acad. Sci. U.S.A.* **2008**, *105*, 3774.
- (4) Nyquist, R. M.; Ataka, K.; Heberle, J. *ChemBioChem* **2004**, *5*, 431. Rich, P. R.; Iwaki, M. *Mol. BioSyst.* **2007**, *3*, 398. Barth, A.; Zscherp, C. *Q. Rev. Biophys.* **2002**, *35*, 369.
- (5) León, X.; Lórenz-Fonfría, V. A.; Lemonnier, R.; Leblanc, G.; Padrós, E. *Biochemistry* **2005**, *44*, 3506.
- (6) Marsh, D. *Biophys. J.* **1999**, *77*, 2630.
- (7) Fraser, R. D. B. *J. Chem. Phys.* **1953**, *21*, 1511.
- (8) Hill, D. G.; Baenziger, J. E. *Biophys. J.* **2006**, *91*, 705.
- (9) Goormaghtigh, E.; Raussens, V.; Ruyschaert, J. M. *Biochim. Biophys. Acta* **1999**, *1422*, 105.
- (10) Pourcher, T.; Bassilana, M.; Sarkar, H. K.; Kaback, H. R.; Leblanc, G. *Philos. Trans. R. Soc. London, Ser. B* **1990**, *326*, 411. Ganea, C.; Fendler, K. *Biochim. Biophys. Acta* **2009**, *1787*, 706.
- (11) Lórenz-Fonfría, V. A.; Padrós, E. *Appl. Spectrosc.* **2005**, *59*, 474.
- (12) León, X.; Leblanc, G.; Padrós, E. *Biophys. J.* **2009**, *96*, 4877.

JA906324Z